

An investigation of annealing and (Zn + Co) co-loading impact on certain physical features of nano-structured (CdO) thin films coated by a sol-gel spin coating process

K. S. Mohammed ^a, J. M. Mansoor ^{a*}, J. Alzanganawee ^a, S. Iftimie ^b

^a“Department of Physics, College of Science, University of Diyala, Iraq

^bFaculty of Physics, University of Bucharest, Bucharest, Romania

Transparent conducting pure and (Co + Zn) co-loaded CdO films were coated by sol-gel spin coating technique with various (cobalt + Zinc) co-loading concentrations. XRD analysis explained the polycrystalline nature of the coated samples with cubic crystal structure along (111) plane being the preferential orientation. The surface morphology and thickness of the prepared thin-films were analyzed by Field Effect Scanning Electron Microscopy (FESEM) and cross-sectional FESEM, respectively. The RMS surface roughness was analyzed by Atomic Force Microscopy AFM measurements. The existence of Cd, Co, Zn, and O elements was confirmed by “Energy-dispersive X-ray Spectroscopy (EDS) spectra”. The red-shift of energy-gap from 2.76 eV to 2.20 eV was carried out by using the Tauc;s and Davis-Mott mathematical relations, in high absorption regions. The shifting from the n-type to p-type semiconductor behavior for the coated samples was estimated by 4 points probe and average Hall coefficient value sign.

(Received April 20, 2021; Accepted September 27, 2021)

Keywords: CdO, Sol-Gel, Co+Zn, Tauc;s and Davis-Mott

1. Introduction

Transparent conducting oxides (TCO_s) such as: Tin, Zinc, Indium, and Cadmium oxides have wide applications in various optoelectronic devices. Of these TCO_s, Cadmium oxide (CdO) have been significantly played an important role with many applications such as photovoltaic-diodes, smart windows, gas sensors, optical wave guides, displays, and transparent-electrodes, etc..., according to high mobility, high carrier concentrations, high conductivity, low resistivity, and high optical transmittance in solar spectrum especially in the visible region [1-3]. Cadmium oxide is an acute toxic (oral, inhalation, and dermal) material but it was used according to its special features and various applications [4]. A variety of thin films coating techniques have been used for the deposition of unloaded, loaded, and co-loaded CdO films “including chemical bath deposition [5][6], pulsed laser deposition [7], vacuum evaporation [8], magnetron sputtering [9], metal organic chemical vapor deposition method” [10], successive ionic layers adsorption, and reaction technique [11], chemical spray pyrolysis[12], and sol gel technique [13]. Among all these, sol-gel spin coating method offers several benefits such as simplicity, the possibility of preparing various large as well as small area coatings, low-cost, homogeneity and high composition controlled way [4, 14]. Cadmium oxide is n - type semiconductor with optical energy-gap value within the range from 2.2 eV to 2.8 eV [4, 15]. Many studies recorded the optoelectronic features of cadmium oxide thin films as unloaded [16, 17], loaded and co-loaded with various metallic ions such as Al [18], In [19], Pb [20], Ga [21], Mn [22], F [23], Co [24], Zn [25], (Zn + F) [3], and (Zn + Co) [26]. Ionic radii is a significant parameter used for choosing appropriate contribution elements [27]; the electrical properties of CdO thin films be controlled as the ionic radius of doping elements being smaller than the ionic radius of Cd⁺² ions [28]. Cobalt (Co) and zinc (Zn) are suitable dopants for CdO lattice because of their lower ionic radius; i.e. Co (0.72Å) and Zn⁺² (0.74Å) than Cd⁺² (0.95Å) [26, 29]. Therefore, the inserting of Co⁺² and Zn⁺² into the cadmium oxide lattice does not cause the tension of CdO lattice to be deformed[30]. Overcome whenever (Co⁺² ions) and (Zn⁺² ions) are substituting the (Cd⁺² ions) or whenever (Co⁺² ions) and (Zn⁺² ions)

* Corresponding author: jasimmansoor13@gmail.com

setup on the interstices locations in the cadmium oxide crystal lattice, they are going to offer additional electrons to CdO crystal structure. In this respect, an increasing of the optical transparency and electrical conductivity of CdO will be predicted [26, 28, 31]. As a consequence from literature review, it was found one work in relation to (Zn + Co) co-doped CdO layers fabricated with perfume atomizer method [26]. In this work, the aim was to (i) study the annealing temperature impact on the optical, structural, morphological, and electrical features of unloaded CdO films and (ii) because there is no work on sol-gel spin coating of (Zn + Co) co-loaded cadmium oxide coated films as of now, our goal was to study the specific impact of (Zn + Co) co-loading levels on the physical features of cadmium oxide prepared samples.

2. Experimental

Unloaded and (Zn + Co) co-loaded CdO thin films have been coated on the substrates through a sol gel spin coating process using Ossila speed controlled (L2001A3-E461-UK) spin coater. (i) For the preparation of the unloaded CdO solutions 0.5M of “cadmium-acetate di-hydrate ($\text{Cd}(\text{CH}_3\text{COO})_2 \cdot 2\text{H}_2\text{O}$)” was dissolved in 2-methoxyethanol and stirred by magnetic stirrer for 20 minutes at 27 °C. (ii) For the preparation of the (Zn + Co) co-loaded mixtures 0.5M of cadmium-acetate di-hydrate ($\text{Cd}(\text{CH}_3\text{COO})_2 \cdot 2\text{H}_2\text{O}$), cobalt chloride ($\text{CoCl}_2 \cdot 6\text{H}_2\text{O}$), and zinc acetate di-hydrate ($\text{Zn}(\text{CH}_3\text{CO}_2) \cdot 2\text{H}_2\text{O}$) were dissolved and mixed in 2-methoxyethanol in order to gain (1+1), (3+3), (5+5), and (7+7) wt% (Zn + Co) co-loaded CdO. Then the mixtures were stirred for 20 min at 27 °C. The temperature of the plate was gradually ramped up to 70 °C then the stabilizer mono-ethanolamine was added drop-by-drop to the solutions. The mixed chemicals of 99% purity were purchased from the Scharlau Company. The obtained solutions and the mixtures were stirred for 2 hours to become homogeneous, transparent, and colorless. The temperature of final solutions and mixtures was reduced to room temperature and filtered by paper-filter, then aged for 24 hours. The prepared solutions and the mixtures were coated on the substrates and the used parameters were 3000 rpm for 40s. The quartz and soda-lime glass (SLG) substrates have been cleaned by acetone, ethanol, methanol, and de-ionized water through ultra-sonication process. The coated thin films were baked at 200°C for 15 minutes on the plate to get rid of the solvents and organic contamination. The procedures from coating to drying were done repeatedly for five times. Finally, the unloaded coated films were post-annealed in the oven at 350, 450, and 550 °C for 1h while the co-loaded thin films were just annealed at 450°C for 1h. The unloaded samples which were annealed at 350, 450, 550 °C and the co-loaded (1+1), (3+3), (5+5), (7+7) wt% (Zn + Co) thin films are denoted in this paper Cd₁, Cd₂, Cd₃, Cd₄, Cd₅, Cd₆, and Cd₇ respectively.

The crystallographic structure of the unloaded and (Zn + Co) co-loaded CdO films was observed by using X-ray diffractometer (XRD Phillips Xpert, Holland, $\lambda_{\text{Cu K}\alpha} = 1.5418740 \text{ \AA}$). The solid angle was varied between 20° and 80°. The optical properties of the coated samples were carried out with UV-Visible (UV-1800, SHMADZU, Japan) spectrophotometer. FE-SEM, cross-section analysis and EDS measurements were performed by using ZEISS Sigma FE-SEMs apparatus. AFM analysis was carried out by TT-2 advanced second generation tabletop microscope. The electrical properties were determined by (ECOPIA HMS-3000VER 3.5, USA) Hall measurements. All measurements were carried out at 27 °C (RT).

3. Results and discussion

3.1. Structural properties

Fig.1a and Fig. 1b represent the XRD analysis of the unloaded and (Zn + Co) co-loaded CdO films. As seen from XRD graphs, all samples have a polycrystalline nature with a cubic structure (*monteponite*) of the CdO. The (111) plane is the preferential growth direction according to (JCPDS card No. 075-0592) except for the unloaded ones which were annealed at 350 °C and showed two preferential orientations intensity at for (111) and (200) planes. Zinc and Cobalt metals, their oxidations forms, or any Co or Zn contribution have not been monitored in the diffraction pattern of the (Zn + Co) co-loaded samples (Fig. 1b Cd₄, Cd₅, Cd₆, and Cd₇). The most

intense peak at (111) plane and other peaks such as; (200), (220) were also detected for all samples except for Cd₁ unloaded thin film. The peak of (311) can be observed for (Zn + Co) co-loaded CdO and unloaded thin films at T=450 and 550 °C and it vanished at T=350 °C, while the peak at (222) plane appeared only for the unloaded sample which was annealed at 550 °C and (7+7) wt% (Zn+Co) co-loaded thin film. The intensity of all peaks for unloaded CdO increases with the (Zn + Co) adding contents, which may indicate that the crystallinity of un-doped CdO increases with co-loading. The increment in the peak intensities with the Annealing temperature confirms the assumption that the crystallinity was enhanced for CdO samples, either due to an increase of the crystallite size[33] or due to the substitutional case of the (Co⁺²ions) and (Zn⁺²ions) with (Cd⁺² ions) attributed to lower ionic radii of the Zn⁺² (0.74Å) Co⁺² (0.72Å) and Co⁺² (0.72Å) [26] than Cd⁺² (0.95Å) [29]. The enhancement in the crystalline structure with annealing temperature and (Zn + Co) co-loading resembles with the previous outcomes for CdO thin films [34, 26, 35].

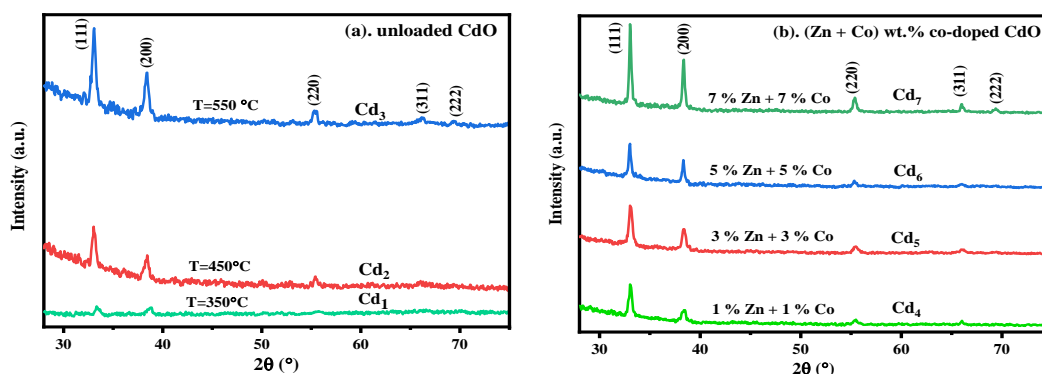


Fig. 1. The XRD pattern of the unloaded and (Zn + Co) co- loaded CdO thin films coated on quartz substrates.

Table 1. Structural parameters of the unloaded CdO films for different annealing temperatures and (Zn + Co) co-loading contributions.

Sample	2θ(°)	FWHM (°)	d-space (Å)	Average Crystallite Size (D) (nm)	Lattice Constant (a)(Å)	Dislocation Density (δ) 10 ¹⁴ lines/m ²	Strain(ε) × 10 ⁻³	Thickness (nm)
Cd ₁	33.45	0.59	2.6786	14.6747	4.6394	4.6436	8.5718	270
Cd ₂	33.03	0.39	2.7112	21.9883	4.6960	2.0683	5.7905	254
Cd ₃	33.07	0.29	2.7086	29.3203	4.6914	1.1632	4.3382	230
Cd ₄	33.09	0.24	2.7070	35.1862	4.6887	0.8077	3.6129	255
Cd ₅	33.07	0.34	2.7084	25.1318	4.6911	1.5832	5.0609	200
Cd ₆	32.99	0.19	2.7151	43.9711	4.7028	0.5172	2.8998	250
Cd ₇	33.04	0.24	2.7111	35.1815	4.6958	0.8079	3.6189	300
JCPDS 075-0592	33.02		2.7105		4.6940			

The crystallite size for (111) peak of the coated films was calculated by usage of “Debye Scherrer’s formula” (1) [3].

$$D = \frac{0.94\lambda}{\beta \cos\theta} \quad (1)$$

where β represents the full width at the half of the maxima, λ (1.5406 Å) is the X-ray wavelength and θ is the Bragg’s angle. The obtained crystallite size (D) for the unloaded CdO continuously

increases with the increasing of the annealing temperatures and (Zn + Co) co-loading contents due to the decreasing of the strain and dislocation density which implies improved crystallinity.

The lattice parameters ($a=b=c$) of a cubic CdO thin films were determined by using the Nelson-Riley function [36] from X-ray diffraction data for all the peaks due to the formula (2) [37].

$$\frac{1}{d^2} = \frac{h^2+k^2+l^2}{a^2} \quad (2)$$

The calculations of the inter planner-spacing (d-space) and lattice constant (a) values for the peaks at (111) plane were in a good agreement with JCPDS file data (075-0592).

The strain values (ε) and the dislocation densities (δ) where estimated by using the following relations (3) and (4),

$$\varepsilon = \frac{\beta \cos \theta}{4} \quad (3)$$

$$\delta = \frac{1}{D^2} \quad (4)$$

The strain values and the dislocation densities were evaluated for the coated thin films from XRD data to find more information about the structural features and they were summarized in Table 1. The values of (ε) and (δ) decreased with the increasing of the annealing temperatures, and for (Zn + Co) co-loading contents the main consequence was an increment in the crystallite size.

3.2 Surface Morphology

The surface morphology of each coated thin film was analyzed for each annealing temperatures for the unloaded CdO coated films and for different (Zn + Co) co-loading concentrations.

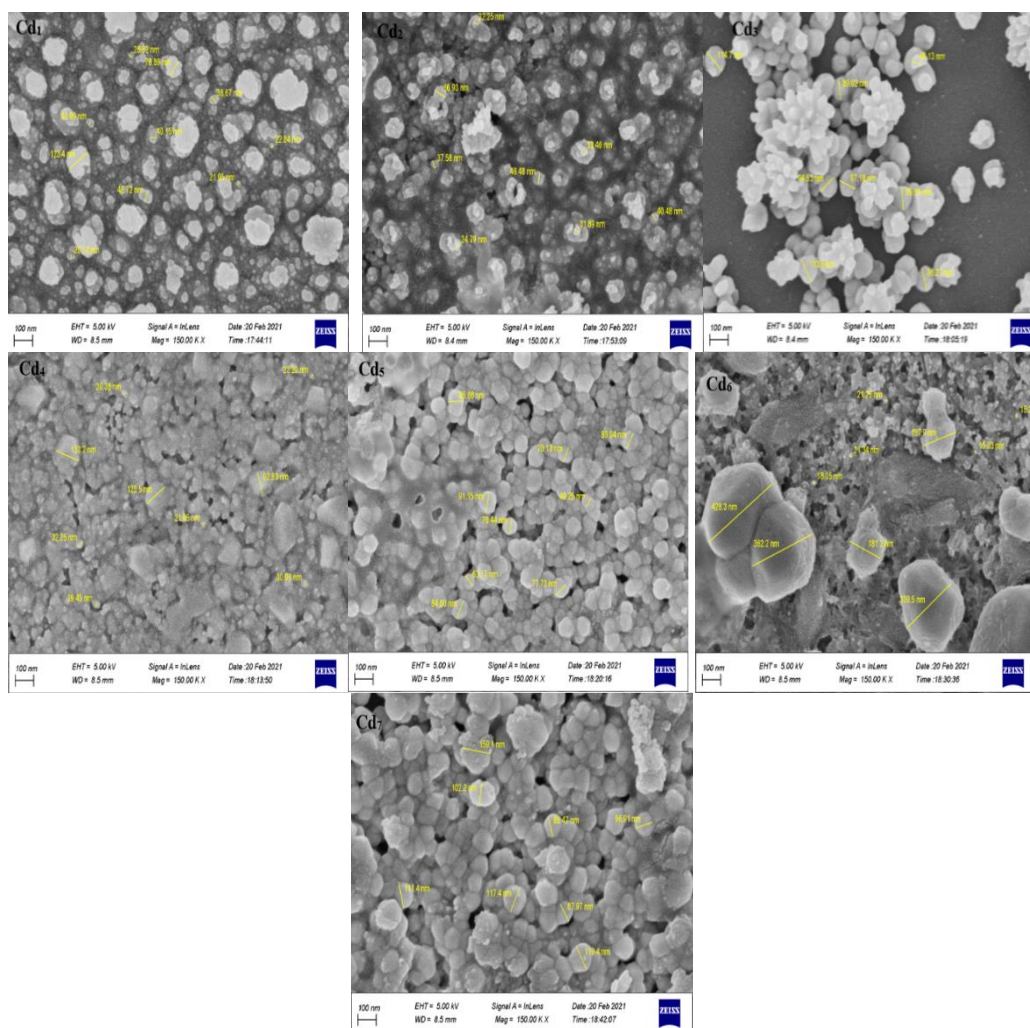


Fig. 2. The FESEM images of the unloaded and (Zn + Co) co-loaded CdO thin films; Cd₁, Cd₂, and Cd₃ pure CdO, Cd₄ (1wt% Zn+1wt% Co), Cd₅ (3wt% Zn+3% Co), Cd₆ (5wt% Zn+5wt% Co), and Cd₇ (7wt% Zn+7wt% Co).co-loaded CdO coated on quartz substrates.

Fig. 2 shows the “FE-SEM images” (unit scale is 100 nm) and the cross-sectional images are illustrated in Fig. 3. The FE-SEM images of the samples Cd₁, and Cd₂, almost show nano-sized spherical granules while the granules like nano-flowers formed by accumulating small granules are observed for Cd₃. The FE-SEM nano-graphs of the samples Cd₄, Cd₅, Cd₆, and Cd₇ almost show cauliflower granules in the surfaces of the coated thin films.

The distribution of granules for the unloaded and (Co + Zn) wt% co-loaded CdO thin films is nearly homogeneous, but deteriorates for the annealed coated film at 550°C (Cd₃) and (5+5) wt% (Zn + Co) co-loading contributions respectively. The average grain size was marginally increased by the increasing of the annealing temperature and (Zn + Co) co-loading levels, which might be related to internal strain caused by a combination of foreign-exchange atoms. The particle morphology for CdO granules is similar to ones in previous works [4, 26, 28]

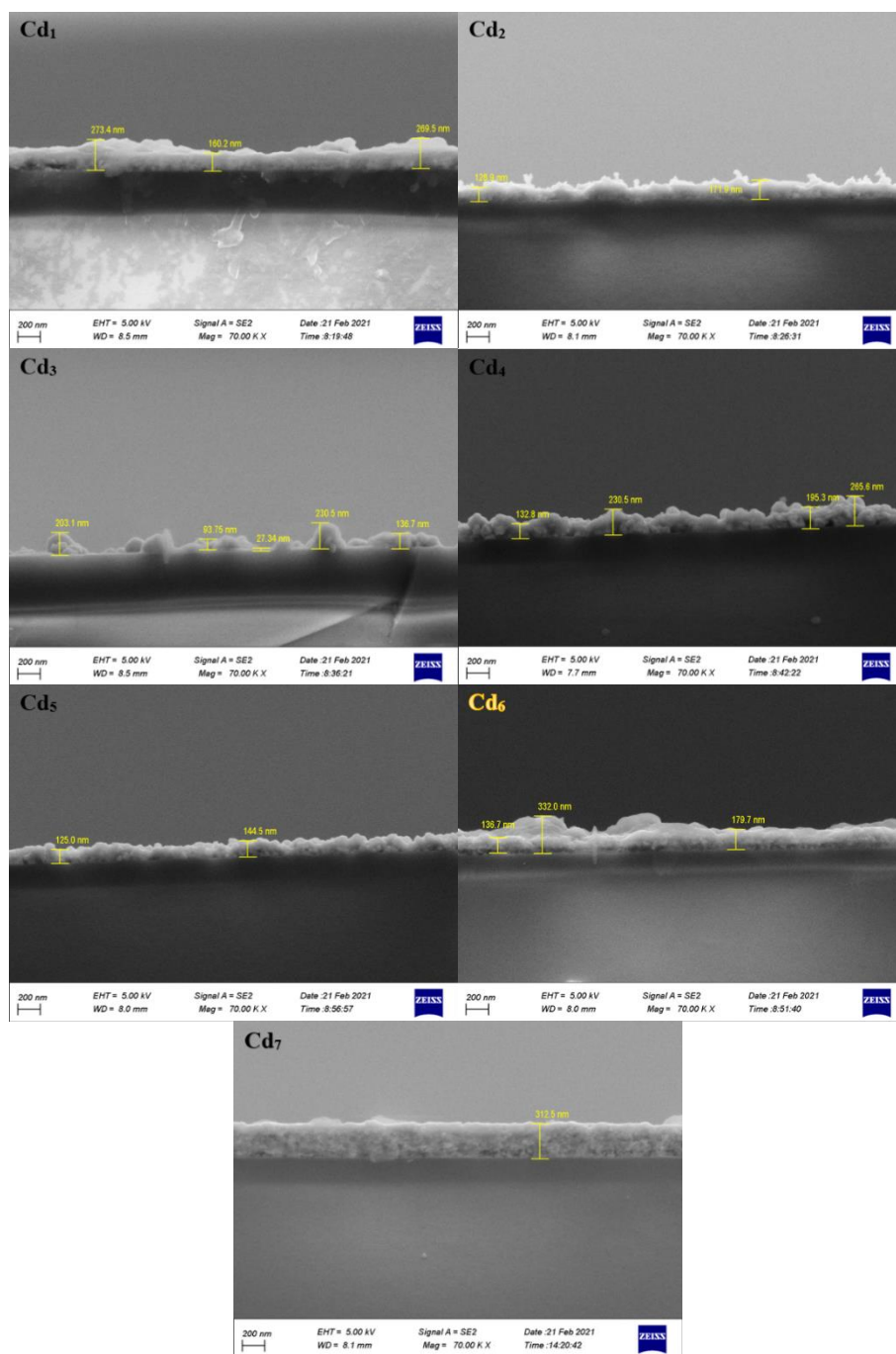


Fig. 3. The cross-sectional FESEM images of the unloaded and (Zn + Co) co-loaded CdO thin films; Cd₁, Cd₂, and Cd₃ pure CdO, Cd₄ (1wt% Zn+1wt% Co), Cd₅ (3wt% Zn+3% Co), Cd₆ (5wt% Zn+5wt% Co), and Cd₇ (7wt% Zn+7wt% Co).co-loaded CdO coated on quartz substrates.

The “cross-sectional FE-SEM images” of the unloaded and (Zn + Co) co-loaded CdO films are shown in Fig. 3. The thickness of the coated films was found to be uniform during the layer, confirming the good adhesiveness with the surface as seen from the diffusion of material into substrate, which could have occurred throughout the annealing process of the coated films. The side shape and the thickness of the coated films have been changed by the variation of the annealing temperature for the unloaded and by the (Zn + Co) co-loading contents for the rest of the samples.

The thickness of the coated thin films was estimated by the “cross-sectional FE-SEM” measurements and was found to be in the range of 200-330. The observed thickness was decreased

with the increment of the annealing temperature for the unloaded CdO films and increased with (Zn + Co) co-loading contributions, and this has as main consequence an increment in the surface roughness [38]. An increment in the surface roughness may causes a diffusion of the incident light, hence reduces the optical transmittance [4].

The representative of EDS spectra of the unloaded and (Zn + Co) co-loaded CdO films are detailed in Fig 4. The elements Cd, O, Co, and Zn were confirmed to be existent in the samples together with other elements such as (Si), which is within the substrate.

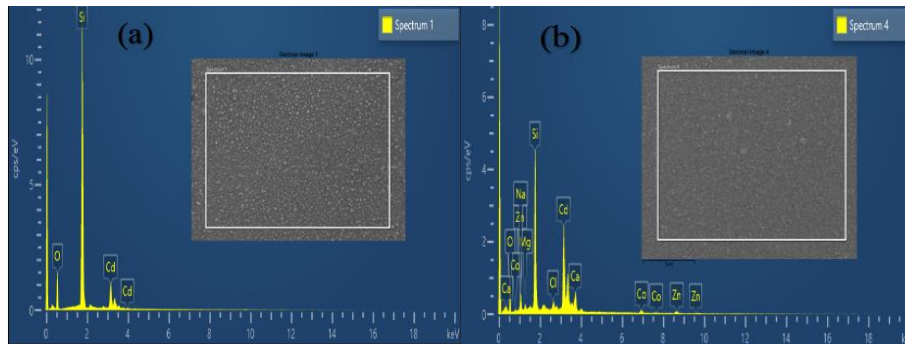


Fig. 4. EDS and electron images analysis of (a) unloaded CdO coated on quartz substrate and (b) (Co + Zn) co-doped CdO film coated on soda-lime glass (SLG) substrate.

EDS spectra reveal that the films are rich in Cd, and no peaks belong to Co_3O_4 or ZnO according to increasing concentrations of Co and Zn. The film deposition process can affect the interaction of ions with the substrate; samples of Cd-rich nature may also be detected by the variance in ionic bond on the surface of substrate.

The surface character of samples (roughness and microstructure) of the unloaded and (Zn + Co) co-loaded CdO films have investigated by AFM study, which is essential for optoelectronic device applications.

Fig. 5 shows the 2- and 3-dimentional AFM surface of the unloaded and (Co + Zn) co-loaded CdO thin films. The surfaces of the films are composed of nano-sized spherical, like nano-flowers and cauli-flowers granules, the granule distributions are similar with the FE-SEM analytics.

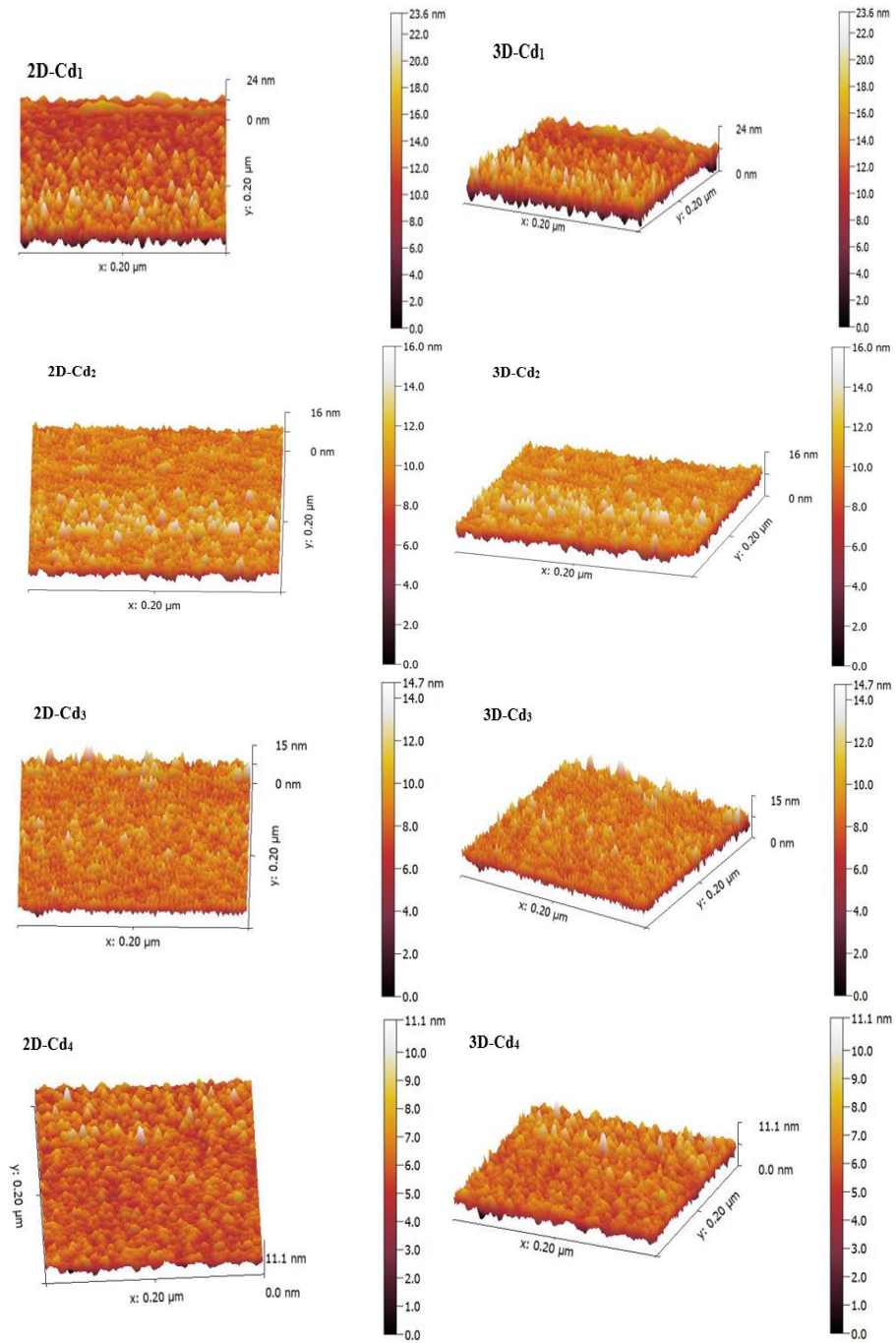


Fig. 5.1 The 2D and 3D AFM images of the unloaded and (Zn + Co) co-loaded CdO thin films; Cd₁, Cd₂, and Cd₃ pure CdO, Cd₄ (1wt% Zn+1wt% Co), Cd₅ (3wt% Zn+3% Co), Cd₆ (5wt% Zn+5wt% Co), and Cd₇ (7wt% Zn+7wt% Co).co-loaded CdO films, coated on quartz substrates.

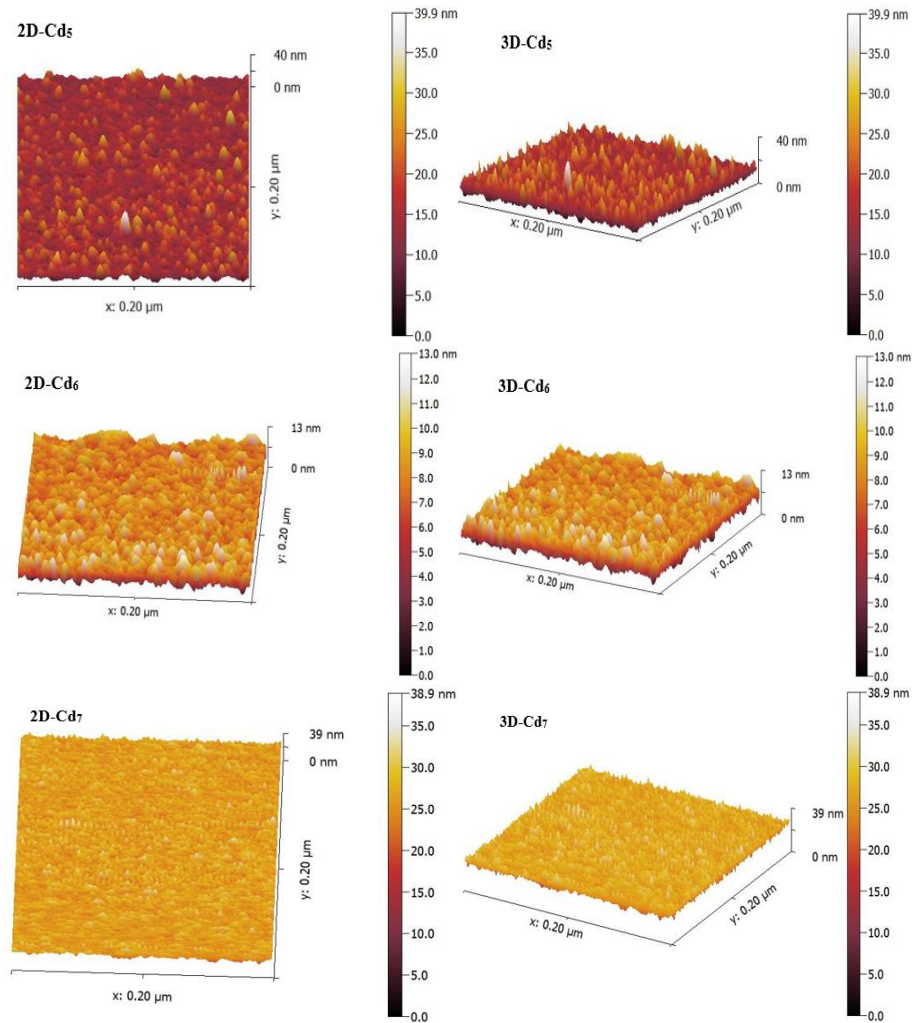


Fig. 5.2 The 2D and 3D AFM images of the unloaded and (Zn + Co) co-loaded CdO thin films; Cd₁, Cd₂, and Cd₃ pure CdO, Cd₄ (1wt% Zn+1wt% Co), Cd₅ (3wt% Zn+3% Co), Cd₆ (5wt% Zn+5wt% Co), and Cd₇ (7wt% Zn+7wt% Co).co-loaded CdO films, coated on quartz substrates.

The RMS roughness and roughness average values for the unloaded CdO films decreased initially and got to the minimum value at T=450°C, then increased with higher annealing temperatures. The roughness average and the RMS roughness values increased with the (Zn + Co) co-loading contributions: these values are shown in Table 2. The structure of the particles seen by AFM images resembles with the ones from earlier works [28, 39]. The FE-SEM and AFM studies reveal that the average granule size of the samples is in the ranges of 10-60 nm and the grain size of the CdO films rises up with the annealing temperature this might be due to the gathering of the granules and, also, for (Zn + Co) co-loading levels may be attributed to the location of Zn or Co at inter-grain locations and interstitial lattice positions.

Table 2. The “roughness average and the root mean square (RMS)” values of the coated thin films.

Sample	Annealing temperature (°C)	(Zn + Co) co-loading levels in CdO (wt%)	Roughness average (nm)	RMS roughness (nm)
Cd ₁	350	0 + 0	4.420	5.621
Cd ₂	450	0 + 0	2.080	2.541
Cd ₃	550	0 + 0	4.282	5.065
Cd ₄	450	1 + 1	2.931	3.489
Cd ₅	450	3 + 3	2.990	3.855
Cd ₆	450	5 + 5	2.153	2.700
Cd ₇	450	7 + 7	6.707	7.856

3.3. Optical Properties

The optical transmittance spectra of the unloaded and (Zn + Co) co-loaded CdO films with different annealing temperatures for the unloaded and (Zn + Co) co-loading concentrations are shown in Fig. 6.(a) and (b), respectively. It can be noticed that the transparency decreased from 90% to 80% with increasing the annealing temperature from 350 to 550°C, but it increases from 85% to 95% with (1+1) wt% (Zn + Co) co-loading contents; this it might be due to the contributions of Zn ions in the CdO:Co lattice and to a better crystallinity, with less point-like defects [40]. Then the transmittance went down in the ranges of 25%-75% with increasing (Zn + Co) co-loading concentrations for a wavelength between 600 and 900 nm; this might be due to the contribution of Zn ions and Co ions in the CdO interstitial or might be attributed to the increment of the scattering from thin film surface or to oxygen deficiencies. The higher absorption can be related to the deformation caused by Co ions in the CdO:Zn lattice [26] and the higher crystallite size values with the decrement of the microstrain values. Computed data from Table 1 support these assumptions.

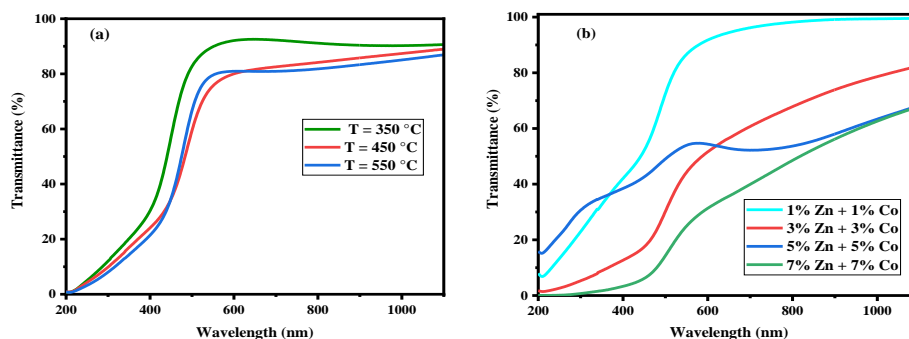


Fig. 6. Optical transmittance of (a) unloaded and (b) (Zn + Co) co-loaded CdO thin films coated on quartz substrates.

The optical absorption of thin films was verified by UV/VIS spectrophotometer and the graphs are drawn in Fig. 7.(a) and 7 (b). As it can be seen from these spectra, the absorption edge of the unloaded CdO is shifted to the larger wavelengths (red shifted) with the increasing of the annealing temperature [41], also red shift was seen for the samples with high percentages of (Zn + Co) co-loading concentrations more than (1+1) wt% (Zn + Co) co-loading contents, e.g. a red shift was demonstrated for high Co loading and (Zn + Co) co-loading contents [42, 26]. The absorbance edge of the unloaded CdO film shifted towards shorter wavelength (blue shifted) with (1+1) wt% (Zn + Co) co-loading contents, this shifting might be attributed to some states that have been populated near the conduction band [43]. The high transmittance and low absorbance of the latter coated sample named Cd₄ which contains (1wt.% Zn+1wt.% Co) co-loaded CdO thin films make them good as an optical window materials for photovoltaic applications.

The optical bandgaps of all prepared thin films is shown in Fig. 8 (a) and 8 (b), and was calculated by the usage of the Tauc's model [44] in the high absorption regions.

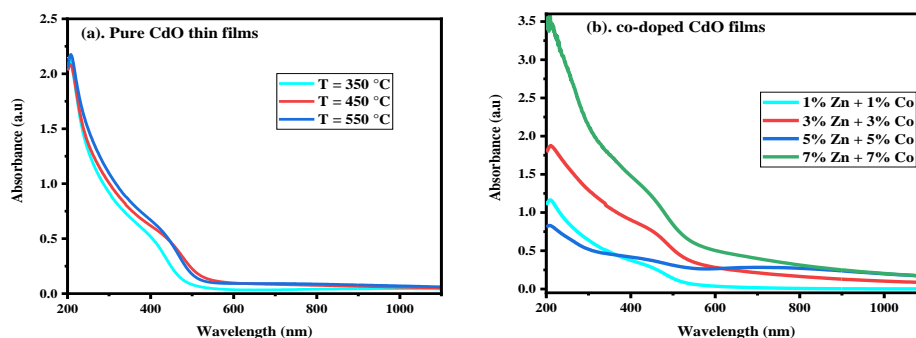


Fig. 7. Variation of absorbance with wavelength for (a) the unloaded and (b) (Zn + Co) co-loaded CdO films coated on quartz substrates.

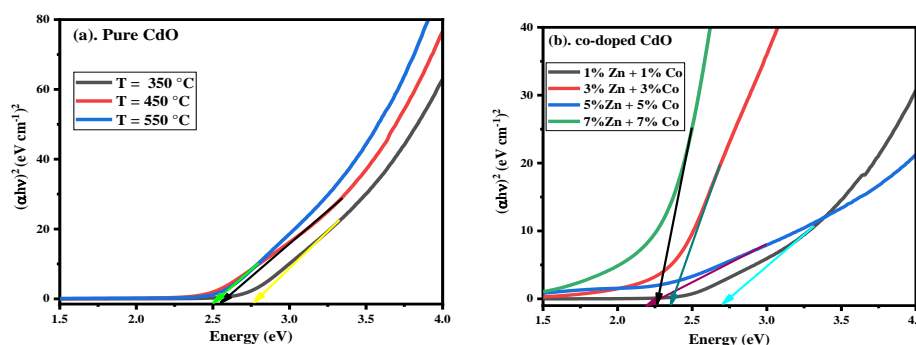


Fig. 8. The $(\alpha hv)^2$ versus (hv) dependence of the (a) unloaded and (b) (Zn + Co) co-loaded CdO films coated on quartz substrates.

$$\alpha hv = A (hv - E_g)^{1/2} \quad (5)$$

where α is the coefficient of absorption, A is a constant, $h\nu$ is the photon energy, and E_g is the optical energy-gap. The energy band-gap values were found to be 2.76, 2.54, and 2.49 for the unloaded samples annealed at $T=350$, 450, and 550°C, respectively, while the energy-gap for the co-loaded CdO films was 2.70, 2.36, 2.20, and 2.27, respectively, for (1+1), (3+3), (5+5), and (7+7) wt% (Zn + Co) co-loading levels. The increased energy-gap values observed for the coated samples might be due to Moss-Burstein Band filling effect [45], and may also be attributed to Vegard's law [46]. The shifting towards the longer wavelengths (red shifted) in the optical energy-gap for the coated samples named Cd₅, Cd₆, and Cd₇ might be attributed to impurity scattering or electron interactions among localized band electrons of (Zn⁺² ions) and (Co⁺² ions) substituted (Cd⁺² ions) [26, 47].

3.4. Electrical Properties

Fig. 9 (a) and Fig 9 (b) illustrate the variation carrier concentration (n), conductivity, resistivity(ρ), Hall mobility (μ), and average Hall coefficient as a function of (Zn + Co) co-loading concentrations in CdO coated thin films. As can be seen, the electrical parameters were strongly influenced by (Zn + Co) co-doping levels, the value of these parameters was shown in Table 3

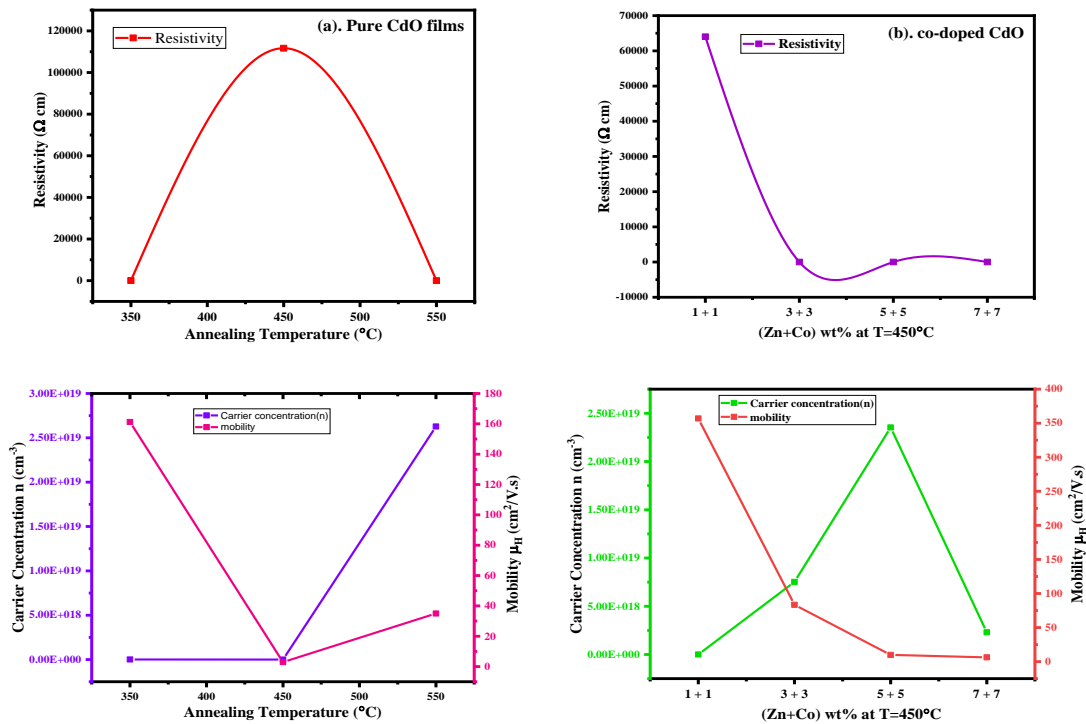


Fig. 9. The carrier concentration, mobility, and the resistivity of (a) the un-loaded and (b) (Zn + Co) co-loaded CdO films coated on quartz substrates.

Table 3. The variation of the electrical parameters of the unloaded and (Co + Zn) co-loaded CdO films.

Sample	(Zn + Co) co-loading levels in CdO (wt%)	Carrier concentration (n) (cm^{-3})	Mobility (μ_H) (cm^2/Vs)	Conductivity ($\Omega^{-1} \text{cm}^{-1}$)	Resistivity (ΩCm)	Average Hall Coefficient (m^2/c)
Cd ₁	0 + 0	4.53×10^{15}	1.61×10^2	1.17×10^{-1}	0.85×10^1	-1.37×10^3
Cd ₂	0 + 0	1.88×10^{13}	0.29×10^1	8.95×10^{-6}	1.12×10^5	-3.32×10^5
Cd ₃	0 + 0	2.63×10^{19}	3.49×10^1	1.47×10^2	6.79×10^{-3}	-2.37×10^{-1}
Cd ₄	1 + 1	2.73×10^{11}	3.57×10^2	1.56×10^{-5}	6.40×10^4	2.28×10^7
Cd ₅	3 + 3	7.52×10^{18}	8.34×10^1	1.01×10^2	9.94×10^{-3}	8.29×10^{-1}
Cd ₆	5 + 5	2.35×10^{19}	0.98×10^1	3.72×10^1	2.68×10^{-2}	-2.65×10^{-1}
Cd ₇	7 + 7	2.30×10^{18}	0.62×10^1	0.23×10^1	4.35×10^{-1}	0.27×10^1

The electrical studies revealed the improvement in the electrical characteristic features of coated CdO thin films by loading with (Zn + Co) co-loading contents. By using hot probe technique at 27 °C and from the sign of average Hall coefficients for both the unloaded and (Zn + Co) co-doped CdO films, it was confirmed that the unloaded samples have n-type conductivity, which shifted to be p-type semiconductors with (Zn + Co) co-loading contributions except the one with (5+5) wt% (Zn + Co) co-loading which possesses n-type semiconducting as seen from the signs of the average Hall coefficient values in Table 3. The enhancement of the electrical features by the increment of the values of the carrier concentrations, mobilities, and conductivities and the decrement in the resistivity values for co-loaded CdO thin films might be attributed to replacement of (Co^{+2} ions) and (Zn^{+2} ions) with the ones of (Cd^{+2} ions) or by the incorporation between either (Co^{+2} ions) and (Zn^{+2} ions) with (O^{+2} ions) which may increase the carrier concentration of the coated films by offering an electron in each incorporation process [3]. On the other hand, the decrement in the resistivity values with (Zn + Co) co-loading might be due to the decreasing of the number of the defects resulting in the enhancement of the crystallinity, which means there was an

improvement in the crystal structure created by the occupancy of Co^{+2} ions and Zn^{+2} ions on the substitutional positions instead of the occupancy on the interstitial ones [48, 49].

4. Conclusions

The unloaded and (Zn+Co) co-loaded CdO thin films were coated through the sol-gel spin coating process. The effects of the annealing temperature and (Zn + Co) co-loading concentrations on the structural, morphological, optical, and electrical features of CdO films were studied. The XRD patterns revealed polycrystalline nature with cubic structure of the coated films which is not really altered through the annealing temperature or by Zn and Co co-loading. The crystallite size increased from 14.67 to 29.32 nm with the increasing of the annealing temperature for the unloaded CdO films and from 21.98 to 43.97 nm with (Zn+ Co) co-loading contents. FE-SEM images showed that the unloaded and the (Zn+Co) co-loaded CdO films have either spherical, like nano-flower, or cauliflower granule shapes. The cross-sectional FE-SEM images indicate the decrease of the surface thickness with annealing temperature for the unloaded CdO films and the increase of it with the (Zn + Co) co-loading level. AFM studies revealed the decrement of RMS surface roughness with the annealing temperature and the increment with (Zn+Co) co-loading contents. EDS spectra confirmed the presence of Cd, and O, in the unloaded samples and, also, confirmed the presence of Cd, O, Co, and Zn elements in the co-loaded CdO thin films.

The optical energy-gap of the unloaded CdO films decreased from 2.76 to 2.49 eV with the increase of the annealing temperature from 350 to 550 °C and the decrease from 2.58 to 2.20 eV with (Zn + Co) co-loading contents, except for (1+1) wt% (Zn + Co) co-loading for which the optical energy-gap increased from 2.58 to 2.70 eV, the latter exhibited high optical transmittance around 90 to 95% in the wavelength range between 600 to 800 nm. Hall Effect measurements revealed that the electrical properties were strongly influenced by co-loading contents. The shifting from n-type to p-type semiconducting was observed for the CdO coated films co-doped with (Zn + Co) contributions. These results of high conductivity and tunable transmittance of (Zn+Co) co-loaded CdO thin films are good candidates for optoelectronic devices, specifically for window layers of solar-cell applications. From all results we conclude that physical features can be enhanced and controlled by annealing temperature and (Zn + Co) co-loading levels.

References

- [1] X. Wu, T. J. Coutts, W. P. Mulligan, *J. Vac. Sci. Technol. A Vacuum, Surfaces, Film* **15**(3), 1057 (1997).
- [2] R. Chandiramouli, B. G. Jeyaprakash, *Solid State Sci.* **16**, 102 (2013).
- [3] M. Anitha, K. Saravanakumar, N. Anitha, L. Amalraj, *Appl. Surf. Sci.* **443**, 55 (2018).
- [4] M. Thirumoorthi, J. T. J. Prakash, *J. Asian Ceram. Soc.* **4**(1), 39 (2016).
- [5] L. R. de León-Gutiérrez, J. J. Cayente-Romero, J. M. Peza-Tapia, E. Barrera-Calva, J. C. Martínez-Flores, M. Ortega-López, *Mater. Lett.* **60**(29–30), 3866 (2006).
- [6] H. Khallaf et al., *Appl. Surf. Sci.* **257**(22), 9237 (2011).
- [7] A. M. Mostafa, A. A. Menazea, *Radiat. Phys. Chem.* **176**, 109020 (2020).
- [8] N. Wongcharoen, T. Gaewdang, T. Wongcharoen, *Energy Procedia* **15**, 361 (2012).
- [9] B. Hymavathi, B. R. Kumar, T. S. Rao, *Procedia Mater. Sci.* **6**(Icmpe), 1668 (2014).
- [10] Z. Zhao, D. L. Morel, C. S. Ferekides, *Thin Solid Films* **413**(1–2), 203 (2002).
- [11] B. Gokul, P. Matheswaran, R. Sathyamoorthy, *J. Mater. Sci. Technol.* **29**(1), 17 (2013).
- [12] M. Anitha, L. Amalraj, N. Anitha, *Appl. Phys. A* **123**(12), 764 (2017).
- [13] R. Kumari, V. Kumar, *J. Sol-Gel Sci. Technol.*, 1 (2019).
- [14] P. Raghu, N. Srinatha, H. M. Mahesh, B. Angadi, in *AIP Conference Proceedings* **1953**(1), 100052 (2018).
- [15] N. Ueda, H. Maeda, H. Hosono, H. Kawazoe, *J. Appl. Phys.* **84**(11), 6174 (1998).
- [16] J. Santos-Cruz et al., *Thin Solid Films* **493**(1–2), 83 (2005).
- [17] D. S. Jbaier, Influence of Annealing on Properties of Cadmium Oxide thin Films Prepared by

- Spray Pyrolysis **33**(8), 1458 (2015).
- [18] M. K. R. Khan et al., *Curr. Appl. Phys.* **10**(3), 790 (2010).
- [19] S. Kose, F. Atay, V. Bilgin, I. Akyuz, *Int. J. Hydrogen Energy* **34**(12), 5260 (2009).
- [20] H. Güney, *Vacuum* **159**, 261 (2019).
- [21] M. Thambidurai, N. Muthukumarasamy, A. Ranjitha, D. Velauthapillai, *Superlattices Microstruct.* **86**, 559 (2015).
- [22] N. Manjula, M. Pugalenth, V. S. Nagarethinam, K. Usharani, A. R. Balu, *Mater. Sci.* **33**(4), 774 (2015).
- [23] M. Anitha, K. Saravanakumar, N. Anitha, L. Amalraj, *Opt. Quantum Electron.* **51**(6), 1 (2019).
- [24] P. Velusamy, R. R. Babu, K. Ramamurthi, E. Elangovan, J. Viegas, M. Sridharan, *Sensors Actuators B Chem.* **255**, 871 (2018).
- [25] H. Güney, D. İskenderoğlu, *Phys. B Condens. Matter* **552**, 119 (2019).
- [26] T. Noorunnisha et al., *Appl. Phys. A Mater. Sci. Process* **126**(10), 1 (2020).
- [27] K. T. R. Reddy, G. M. Shanthini, D. Johnston, R. W. Miles, *Thin Solid Films* **427**(1–2), 397 (2003).
- [28] G. Turgut, *J. Mater. Sci. Mater. Electron.* **28** (22), 16992 (2017).
- [29] N. N. Greenwood, A. Earnshaw, *Chemistry of the Elements*. Elsevier, 2012.
- [30] G. Turgut, *Thin Solid Films* **594**, 56 (2015).
- [31] K. Usharani, A. R. Balu, *Acta Metall. Sin. English Lett.* **28**(1), 64 (2015).
- [32] A. M. El Sayed, A. Ibrahim, *Mater. Sci. Semicond. Process* **26**, 320 (2014).
- [33] I. Ben Miled et al., *J. Sol-Gel Sci. Technol.* **83**(2), 259 (2017).
- [34] M. A. Rahman, M. K. R. Khan, *Mater. Sci. Semicond. Process* **24**, 26 (2014).
- [35] K. V. Kannan Nithin, M. R. M. Krishnappa, *J. Phys. Conf. Ser.* **1362**(1), 2019.
- [36] J. B. Nelson, D. P. Riley, *Proc. Phys. Soc.* **57**(3), 160 (1945).
- [37] J. R. Villalobos-Hernandez, C. C. Müller-Goymann, *Int. J. Pharm.* **322**(1–2), 161 (2006).
- [38] Y.-P. Zhao, R. M. Gamache, G.-C. Wang, T.-M. Lu, G. Palasantzas, J. T. M. De Hosson, *J. Appl. Phys.* **89**(2), 1325 (2001).
- [39] M. Benhaliliba et al., *J. Lumin.* **132**(10), 2653 (2012).
- [40] C. Ravichandran, G. Srinivasan, C. Lennon, S. Sivananthan, J. Kumar, *Superlattices Microstruct.* **49**(5), 527 (2011).
- [41] A. H. O. Alkhayatt, I. A. D. Al-hussainy, O. A. C. Al-rikaby, *Adv. Phys. Theor. Appl.* **34**, 1 (2014).
- [42] S. Sönmezoğlu, T. A. Termeli, S. Akin, I. Askeroğlu, *J. Sol-Gel Sci. Technol.* **67**(1), 97 (2013).
- [43] I. Jacques, Pankove, *Optical Processes in Semiconductors*, New York: Dover publication institute, 1971.
- [44] J. Tauc, R. Grigorovici, A. Vancu, *Phys. status solidi* **15**(2), 627 (1966).
- [45] E. Burstein, *Phys. Rev.* **93**(3), 632 (1954).
- [46] L. M. Guia, V. Sallet, S. Hassani, M. C. Martínez-Tomás, V. Muñoz-Sanjose, *Cryst. Growth Des.* **17**(12), 6303 (2017).
- [47] I. Hamberg, C. G. Granqvist, *J. Appl. Phys.* **60**(11), R123 (1986).
- [48] S. W. Shin et al., *Surf. Coatings Technol.* **231**, 364 (2013).
- [49] N. Manjula, A. R. Balu, K. Usharani, N. Raja, V. S. Nagarethinam, *Optik (Stuttg.)* **127**(16), 6400 (2016).